PLOS ONE

RESEARCH ARTICLE

Medication-related osteonecrosis of the jaws after tooth extraction in senescent female mice treated with zoledronic acid: Microtomographic, histological and immunohistochemical characterization

Claudia Cristina Biguetti[1☯]*, André Hergesel De Oliva[1‡], Kent Healy[2‡], Ramez Hassan Mahmoud[1‡], Isabela Do Carmo Custódio[3‡], Dulce Helena Constantino[3‡], Edilson Ervolino[1‡], Marco Antonio Hungaro Duarte[4‡], Walid D. Fakhouri[2‡], Mariza Akemi Matsumoto[1☯]

1 Department of Basic Sciences, São Paulo State University (UNESP) - School of Dentistry, Araçatuba, São Paulo, Brazil, **2** Department of Diagnostic and Biomedical Sciences, University of Texas Health Science Center at Houston, Houston, Texas, United States of America, **3** Department of Health Sciences Universidade Sagrado Coração – USC, Bauru, São Paulo, Brazil, **4** Department of Endodontics, São Paulo University – FOB/USP, Bauru, São Paulo, Brazil

☯ These authors contributed equally to this work.
‡ These authors also contributed equally to this work.
* claudiabiguetti@hotmail.com

OPEN ACCESS

Citation: Biguetti CC, De Oliva AH, Healy K, Mahmoud RH, Custódio IDC, Constantino DH, et al. (2019) Medication-related osteonecrosis of the jaws after tooth extraction in senescent female mice treated with zoledronic acid: Microtomographic, histological and immunohistochemical characterization. PLoS ONE 14(6): e0214173. https://doi.org/10.1371/journal.pone.0214173

Editor: Dominique Heymann, Universite de Nantes, FRANCE

Received: March 5, 2019

Accepted: May 7, 2019

Published: June 14, 2019

Data Availability Statement: All relevant data are within the manuscript and its Supporting Information files.

Funding: This work was supported by ICC -scholarship number #2018/19409-0, from Fundação de Amparo à Pesquisa do Estado de São Paulo (FAPESP) - http://www.fapesp.br/ MAM - grants #2013/04714-8 and #2019/10355-7 from

Abstract

Treatment with cumulative dosages of zoledronic acid (ZA) in elderly patients is a risk factor for the development of medication-related osteonecrosis of the jaws (MRONJ), mainly related to surgical triggers such as tooth extraction. However, animal models for the investigation and understanding of MRONJ pathophysiology in senescent and postmenopausal stages remains to be developed and characterized. The aim of this study was to analyze MRONJ development in senescent female mice treated with cumulative dosages of ZA. For this purpose, twenty 129/Sv female mice, 64 weeks old, were treated with 0.9% saline solution as control group (n = 10), and with ZA at 250μg/Kg (n = 10), once a week, starting 4 weeks before the upper right incisor extraction and until the end of the experimental time points (7 days and 21 days). At 7 and 21 days post-surgery, specimens were harvested for microCT, histological, birefringence and immunohistochemical analysis. Clinically, an incomplete epithelialization was observed in ZA group at 7 days and a delayed bone matrix mineralization and collagen maturation at 7 and 21 days compared to the controls. Controls revealed sockets filled with mature bone at 21 days as observed by microCT and birefringence, while ZA group presented delayed bone deposition at 7 and 21 days, as well increased leukocyte infiltration and blood clot at 7 days, and increased bone sequestrum and empty osteocyte lacunae at 21 days ($p<0.05$). Also, ZA group presented decreased quantity of TGFb+ and Runx-2+ cells at 7 days, and decreased quantity of TRAP+ osteoclasts compared to the control at 21 days ($p<0.05$).

Fundação de Amparo à Pesquisa do Estado de São Paulo (FAPESP) - http://www.fapesp.br/ WDF - grant# R15GM122030-01 from National Institutes of Health (NIH) - https://www.nih.gov/.

Competing interests: The authors have declared that no competing interests exist.

Altogether, these data demonstrate the usefulness of this model to understanding the pathophysiology of MRONJ.

Introduction

The chronic use of antiresorptive drugs, such as nitrogen-containing bisphosphonates (nBP's), is a risk factor in medication-related osteonecrosis of the jaw (MRONJ), and has been clearly associated with the disease onset [1–3]. MRONJ is a pathological condition characterized by a non-viable exposed maxillary or mandibular bone in the oral cavity in patients with previous or ongoing antiresorptive therapy with the exception of previous radiation treatment [1]. Risk factors of MRONJ include invasive dental procedures involving bone injuries, whereby dental extraction is the most common triggering factor [4, 5]. Furthermore, other procedures that require bone manipulation, such as dental implants, have a comparable risk to that of dental extractions [2, 6]. Additional comorbidities and systemic conditions have been reported as frequently associated with risk of developing MRONJ (i.e., cancer, advanced age, and the use of immune suppressive medications) [1, 2]. Other predisposing risk factors include drug dosage [7], potency, route of administration, and duration of nBP treatment [1, 6]. Notably, zoledronic acid (ZA) is 100 to 1000-fold more potent than other nBP's [8], and therefore it is the first choice for the treatment of patient with bony metastasis [9]. It is also a highly effective drug for severe postmenopausal osteoporosis in elderly women [10], thereby reducing the risk of vertebral and hip fractures by up to 70% and 41%, respectively [11].

While MRONJ has well-defined histopathological characteristics, its pathophysiological mechanism remains to be fully elucidated [1]. MRONJ human biopsies exhibit empty osteocyte lacunae, lack of osteoblasts along new bone, and detached osteoclasts. MRONJ biopsy samples are frequently associated with a secondary infection [12, 13], and may exhibit similar histological characteristics to osteomyelitis and osteoradionecrosis [13]. Previous studies have explored MRONJ animal models to provide explanations for the disease process. Hypotheses examined in these studies include over-suppression of osteoclasts bone resorption in the jaws, more than in endochondral bones [14], angiogenesis inhibition [15, 16] and more recently, alterations of innate and adaptive immune responses [17, 18].

It is important to emphasize that bone healing depends on the initial inflammatory response, which can be affected by the type drug and the compromised bone cells in the injured areas [19]. Therefore, an immunological mechanism involved in the development of MRONJ is an important process that needs further investigation using a suitable animal model. Mice are considered a reliable *in vivo* system for immunological investigations and have conferred multiple advantages over other animal models therein [20]. Namely, the small size of the animal requires reduced amount of the drug, rapid cumulative effects due to rapid mice metabolism, and the possibility of using genetically-manipulated animals to determine a cause-and-effect relationship between the target disruption of a gene and its function [21–23]. The vast majority of MRONJ models have been developed using mainly C57BL/6 and other mice strains (S1 Table), [15, 17, 23–39]. The C57BL/6 is the most widely used inbred strain and with a large source of genetically modified lines [40]. However, C57Bl/6 mice have overall less bone volume than other strains, like 129Sv mice [41]. Therefore, the use of 129Sv could provide an advantage on C57Bl/6, as a mouse strain with more robust bone for studying conditions where bone density is an important variable, such as bone healing and MRONJ models.

The majority of previous studies reported the use of ZA via IP (intraperitoneal) or IV (intravenous) administration as an antiresorptive medication of choice for inducing MRONJ lesions in mice [15, 17, 24, 25, 27, 29, 30, 32, 33, 35, 37, 39, 42–46], considering its higher potency when compared to other IV or oral nBP's [47]. Moreover, all mouse studies presented in S1 Table were performed in young or adult animals (age varying from 6 to 16 weeks old). The age of the tested mice is an important variable that possibly increases the risk for MRONJ onset. According to the last clinical update from AAOMS [3] the risk of developing MRONJ among osteoporotic patients exposed to nBPs remains very low, but affects mainly the population over the age of 55. The average age of menopaused women is 51 years old, and they can live 30% of their life in a postmenopausal state, considering a life expectancy of 80 years old approximately [48]. Considering these epidemiological and clinical data, senescent female mice could provide a suitable model to investigate bone healing after dental procedures in this treatment conditions, using ZA or other MRONJ potential drugs. Thus, the aim of this study is to analyze bone healing after tooth extraction in senescent mice treated with cumulative doses of ZA, and investigate whether 129Sv senescent female mice are appropriate model by inducing and understanding the MRONJ development via microtomographic, histopathological and immunohistochemical characterization.

Material and methods

In vivo assays

In vivo assays were performed by using a total of twenty 129 S/v female mice (60-weeks-old), provided by the animal facilities of University of Sao Paulo (University of São Paulo, Ribeirão Preto, São Paulo, Brazil) and maintained in the animal facilities of the Universidade Sagrado Coração, Bauru, São Paulo, Brazil). Animals were handled according to the recommendations in the Guide for the Care and Use of Laboratory Animals of the National Institutes of Health (Institute of Laboratory Animal Resources (U.S.). The experimental protocol was performed according to ARRIVE guidelines [49] and approved by the local Institutional Committee for Animal Care and Use of the Universidade Sagrado Coração (CEUA Protocol number #9589271017). First, estrus cycle was evaluated by vaginal cytology following previous recommendation and criteria for stained vaginal smears with Toluidine blue O stain [50, 51]. Sixty-weeks old mice presented cytology with predominance of leukocytes and few epithelial cells for four consecutive weeks, indicating a persistent diestrum and were considered in the post-menopausal period. At 64 weeks old, the mice were divided into control (n = 10) and experimental (n = 10). The Control group was treated with IP injection of 0.01ml of sterile 0.9% saline solution; while the ZA group was treated with an IP injection of Zoledronic Acid (Merck KGaA, SML0223, Darmstadt, Germany) at 250 μg/kg diluted in 0.9% sterile solution once a week. Mice received IP injections of ZA once a week, starting 4 weeks before tooth extraction and continuing until the end of experimental periods (7 days or 21 days). Animals were fed with sterile standard solid mice chow (Nuvital, Curitiba, PR, Brazil) and sterile water, except on the first 72 hours after surgery, in which diet was soft for postoperative recovery and to facilitate the ingestion of food. Animals were clinically monitored and controlled regarding body loss, feeding and behavior. No antibiotics or anti-inflammatory drugs were administered to the animals after tooth extraction, in order to avoid interference with investigated inflammatory pathways [22]. Experimental groups were comprised of 5 animals per group/time point (7 and 21 days), and specimens were harvested for microCT, histological, birefringence and immunohistochemical analysis.

Mice tooth extraction model

Tooth extractions were performed as previously described [52, 53]. Animals received general anaesthesia by intramuscular administration of ketamine chloride (80 mg/kg) (Dopalen, Agribrans do Brasil LTDA, SP, Brazil) and xylazine chloride (15 mg/kg) (Anasedan, Agribrands do Brasil LTDA, SP, Brazil). Each mouse's oral cavity was divided into two parts: upper right side with extraction (E side), and upper left side without extraction (NE side). Then, the right upper incisor luxation was performed with a dental exploratory probe until the tooth became mobile, and was then removed delicately with forceps. Importantly, samples with root fractures and with the presence of apical stem cell niche (visualized under the surgical microscope immediately after surgery) were not included in the study, as also characterized as the criteria for samples inclusion/exclusion in previous studies [52, 53]. At the end of experimental time points, mice were euthanized, and maxillae containing the socket area were harvested. Additionally, femur and L5 vertebrae were collected for supplementary analysis at the experimental period of 7 days (after 5 doses of ZA). Bone specimens were immediately fixed in PBS-buffered formalin (10%) solution (pH 7.4) for 48h at room temperature, subsequently washed overnight in running water and maintained temporarily in alcohol fixative (70% hydrous ethanol) and scanned for μCT analysis, and then decalcified in 4.13% EDTA (pH 7,2) for histological processing.

Micro CT analyses

Bone specimens were scanned by the Skyscan 1174 System (Skyscan, Kontich, Belgium) at 50 kV, 800 μA, with a 0.5 mm aluminium filter, 180 degrees of rotation and exposure range of 1 degree and a resolution of 14μm pixel size. Subsequently, images were reconstructed using the NRecon software, following three-dimensional (3D) reconstruction of the images using CTVox, and the quantitative parameters were assessed using CTAn software. For the quantitative analyses, guidelines of μCT characterization were used as previously described [54]. The NE side maxilla and E side for the newly bone formed in the extracted alveolar area were analyzed following microtomographic parameters reported in previous studies [52]. Briefly, fraction of bone volume (BV/TV, %) was measured considering the region of the alveolar process of the upper incisor facing the animal palate, in a region of interest (ROI) of 1mm length and a diameter of 0.9 mm, as demonstrated later in the results. For the newly bone formed in the extracted alveolar area, BV/TV (%) was measured in a segmented in a cylindrical ROI covering the entire length of the alveolus (3mm) and a diameter of 1 mm.

Histology sample preparation

Maxillary bone specimens were immersed in buffered 4% EDTA for demineralization for 3 weeks, then the specimens underwent histological processing for embedding in paraffin blocks. Transversal serial 5μm histological slices from coronal and medial third were cut for histological staining with H&E, modified Goldner's Trichrome/Alcian Blue, and Picrosirius Red.

Histological and histomorphometric analysis

A qualitative histopathological analysis was performed considering parameters of healing and MRONJ. Histomorphometric analysis was performed using a total of eight technical sections from middle regions of the alveolar socket stained by H&E. These samples were used to quantify the following components: blood clot, inflammatory infiltrate, blood vessels, osteocytes and empty lacunae. Quantification of histological parameters was performed by a single

calibrated investigator with a binocular light microscope (Olympus Optical Co., Tokyo, Japan) using a 100× immersion objective. Eight histological fields per H&E stained section, comprising the region of alveolar socket were captured using a 100× immersion objective. A grid image was superimposed on each histological field, with ten parallel lines and 100 points in a quadrangular area, by using Image J software (Version 1.51, National Institutes of Health, Bethesda, Maryland, USA). Only the points coincident with the histological parameters were considered and the total number of points was obtained to calculate the area density for each healing component in each section [22].

Modified Goldner's Trichrome/Alcian Blue

Modified Goldner's Trichrome/Alcian Blue (GT+ Alcian Blue) was used to stain newly formed bone matrix and cartilage with green and dark blue color, respectively. Hematoxylin was used as a counter stain for nuclei. Particularly, this stain offers a wider array of colors and contrast, for a clearly differentiation between the different inflammatory cells and bone components. Histological sections were incubated for 30 min at 56 ˚C, followed by washing in distilled water for 5 min. Then, the sections were stained with Alcian Blue for 15 minutes, and washed 3 times with distilled H_2O for 3 min each time. Subsequently, sections were stained with Hematoxylin Harris for 45 seconds, rinsed in tap water for 6 minutes and distilled water for 5 minutes. Then, sections were stained in Fuchsin-Ponceau solution for 30 minutes, rinsed in 1.0% acetic acid solution for 1 minute, then stained in Orange G dye for 8 minutes, rinsed again in 1.0% acetic acid solution for 1 minute, stained in Light Green solution for 20 minutes, and finally rinsed in 1.0% acetic acid solution for 1 minute. Lastly, the slides were dehydrated in ascending ethanol solution followed by 2 washes in xylene for 3 min each time, and mounted with mounting media.

Birefringence analysis for collagenous content maturation

For analyzing the quality and quantity of collagen, birefringence analysis was performed with Picrosirius-polarization method. For this method, eight histological sections from central region of the each alveolar socket were stained with Picrosirius Red stain and the images of 4 histological fields a 40× objective were captured by a polarizing lens coupled to a binocular inverted microscope (Leica DM IRB/E), as previously described [55]. Only socket area filled with new tissue was considered in this analysis. At the beginning, spectra of green, yellow and red colors were defined, followed by RGB (red, blue, green) values for each color spectrum and the quantity of pixels2 of each color correspondent to each field. Afterwards, the mean pixels2 values considering the intensity of birefringence brightness ($pixels^2$) was performed using the AxioVision 4.8 software (Carl Zeiss) to define total area of green (thin and immature fibers), as well yellow and red collagen fibers (thicker and mature).

Immunohistochemistry and immunofluorescence

Bone sections from socket areas at 7 and 21 days post tooth extraction were deparaffinized following standard procedures. For immunohistochemistry, slices were pre-incubated with 3% hydrogen peroxidase block (Spring Bioscience Corporation, CA, USA) and subsequently incubated with 7% NFDM to block serum proteins. For the central regions of sockets, sections were incubated with goat polyclonal anti-Runx2 (sc8566, Santa Cruz Biotechnology, Carpinteria, USA), rabbit polyclonal anti-F4/80 (sc26643, Santa Cruz Biotechnology, Carpinteria, USA) at a concentration of 1:100, and rabbit polyclonal anti-TGF-β (sc7892, Santa Cruz Biotechnology, Carpinteria, USA), goat polyclonal anti-TRAP (sc30832, Santa Cruz Biotechnology, Carpinteria, USA), at a concentration of 1:200, for 1h at room temperature. For detection

methods, universal immuno-enzyme polymer method was used and sections were incubated in immunohistochemical staining reagent for 30 min at room temperature. For detection of antigen–antibody we used 3–3'-diaminobenzidine (DAB), followed by counter-staining with Mayer's hematoxylin. For control staining of the antibodies, serial sections were treated only with the Universal immuno-enzyme polymer, in a separate preparation. Immunofluorescence was performed following protocols previously described [56, 57]. For detection of cell proliferation in the oral mucosa, sections from the initial portions of sockets were incubated with primary antibody for Proliferating Cell Nuclear Antigen (PCNA) (#MAB424, Merck Millipore, Darmstadt, Germany) diluted to 1:150 in blocking solution and incubated at 4˚C overnight. After washing steps in 1×PBS (3 times, 10 min each wash), the sections where incubated with Cy3 secondary antibody (#715-165-150, Jackson ImmunoResearch Laboratories, West Grove, PA, USA), diluted to 1:200 in blocking solution, during 2 hours in a dark chamber at room temperature. Then the sections were washed 3 times in 1×PBS (10 min each wash) and the nuclei were counter-stained with DAPI (D9542-50, Sigma-Aldrich Corp., St. Louis, MO, USA) for 10 minutes of incubation in a dark chamber. After the last washing step in 1×PBS for 10 min, the slides were mounted with ProLong Gold Antifade Reagent (P36930, Life Technologies, Carlsbad, CA, USA).

Quantification of TRAP, Runx-2 and F4/80 immunolabeled cells

The analysis of immunolabeled TRAP, Runx-2 and F4/80 was performed following the similar criteria described previously for histomorphometric analysis and as previously reported [53]. Briefly, a biological replicate of five samples for each experimental period and strains were used for quantitative analysis. A total of 3 sections of each sample containing the central region of the alveolar socket were used for targets quantification [53]. A total of eight fields were analyzed by using Image J software (Version 1.51, National Institutes of Health, Bethesda, Maryland, USA). Only the points coincident with the immunolabeled cells were considered in cell counting and the mean for each section was obtained for statistical analysis.

Statistical analysis

Quantitative data were statistically analyzed for distribution of normality using Shapiro-Wilk and D'Agostino-Pearson omnibus test. For data with normal distribution, multiple comparisons among data were analyzed by One-Way analysis of variance (ANOVA) followed by the Tukey post-test. For data that did not fit in the normal distribution, the Mann-Whitney and Kruskal-Wallis test were used followed by the Dunn's test. The alpha level for all tests was set to (5%), then $p<0.05$ were considered statistically significant. Data sets are presented with descriptive statistics, containing mean and standard deviation. All statistical tests were performed using the GraphPad Prism 5.0 software (GraphPad Software Inc., San Diego, CA, USA).

Results

Given the advantages for using a mouse as an animal model for immunological studies, our primary interest in this study was to investigate the bone healing in senescent and postmenopausal 129 Sv female mice treated with ZA, in order to provide a tool for understanding the MRONJ pathophysiology. Before we induced MRONJ through tooth extraction, we characterize the senescence and postmenopausal state in the female mice. The animals were evaluated for estrous cycle and presented a predominance of leukocytes and few epithelial cells for 4 consecutive weeks, indicating a persistent diestrum and a postmenopausal state (Fig 1A). At 64

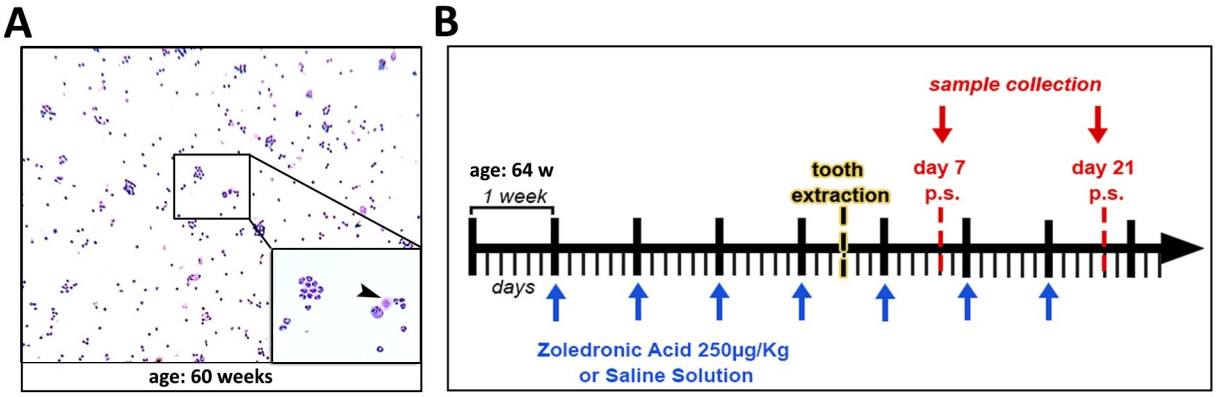

Fig 1. Experimental design of MRONJ model in senescent female 129 Sv mice. A) Vaginal smears with Toluidine blue O stain showing predominance of leucocytes and few nucleated epithelial cells (arrow head) for 4 consecutive weeks, as indicated for 60 weeks of age. B) Schematic timeline for control and ZA groups: mice were treated with 0.9% saline solution or ZA at a dosage of 250µg/Kg, starting 4 weeks before tooth extraction.

https://doi.org/10.1371/journal.pone.0214173.g001

weeks old, control and ZA group mice began receiving IP injections of each substance, 0.9% saline solution or ZA, respectively (Fig 1B).

Oral mucosal evaluation

At 68 weeks old, right upper incisor was atraumatically extracted four weeks after the initial IP injection with both solutions (S1A Fig). The animals were monitored daily for clinical post-operative symptoms or signs of infection or distress. At 7 days post-operation, 100% of control group presented a complete healing of the oral mucosal, covering the surgical wound. On the other hand, 40% of ZA group clinically presented delayed epithelial socket closure. However, 100% of mice of control and ZA group mice presented a complete mucosal closure at 21 days (S1B Fig).

Microtomographic analysis of E site and NE site maxillary bone

After euthanasia, maxillae from 7 and 21 days post extraction were collected for initial microtomographic qualitative and quantitative analyses. Extant bone and new bone formation were analyzed at NE sites (Fig 2A and 2A') and E sites (Fig 2B and 2B'), respectively. On the NE sites, the cumulative effects of ZA administration are evident in the significant increase in BV/TV of alveolar ridges in the ZA group compared to the control group. On the NE sites, at 7 days post tooth extraction (or 5 injections of ZA or vehicle), the ZA group presented 86.67 ± 6.10% of BV/TV compared to 78.25 ± 9.74% of the control group. At 21 days post tooth extraction (or 7 injections of ZA or vehicle), the ZA group presented 91.67 ± 1.52% of BV/TV compared to 72.00 ± 16.10% of the control group (Fig 2A and 2A'). Regarding the newly formed bone in the alveolar sockets post tooth extraction (E sites), no significant differences were observed at 7-day time point between both groups. In comparison, both groups (Control and ZA) presented gradual bone apposition, with significant increased values of BV/TV compared to the initial time point at 21 days. In the comparison between groups, control group presented significant increased bone formation compared to ZA, with 55.82 ± 3.51% vs. 44.45 ± 4.96% (Fig 2B and 2C).

Birefringence birefringence analysis for collagen evaluation

Using birefringence analysis, we evaluated the quality and quantity of collagen in new bone formed after tooth extraction in E sites (Fig 3A–3E). The transversal sections containing sites

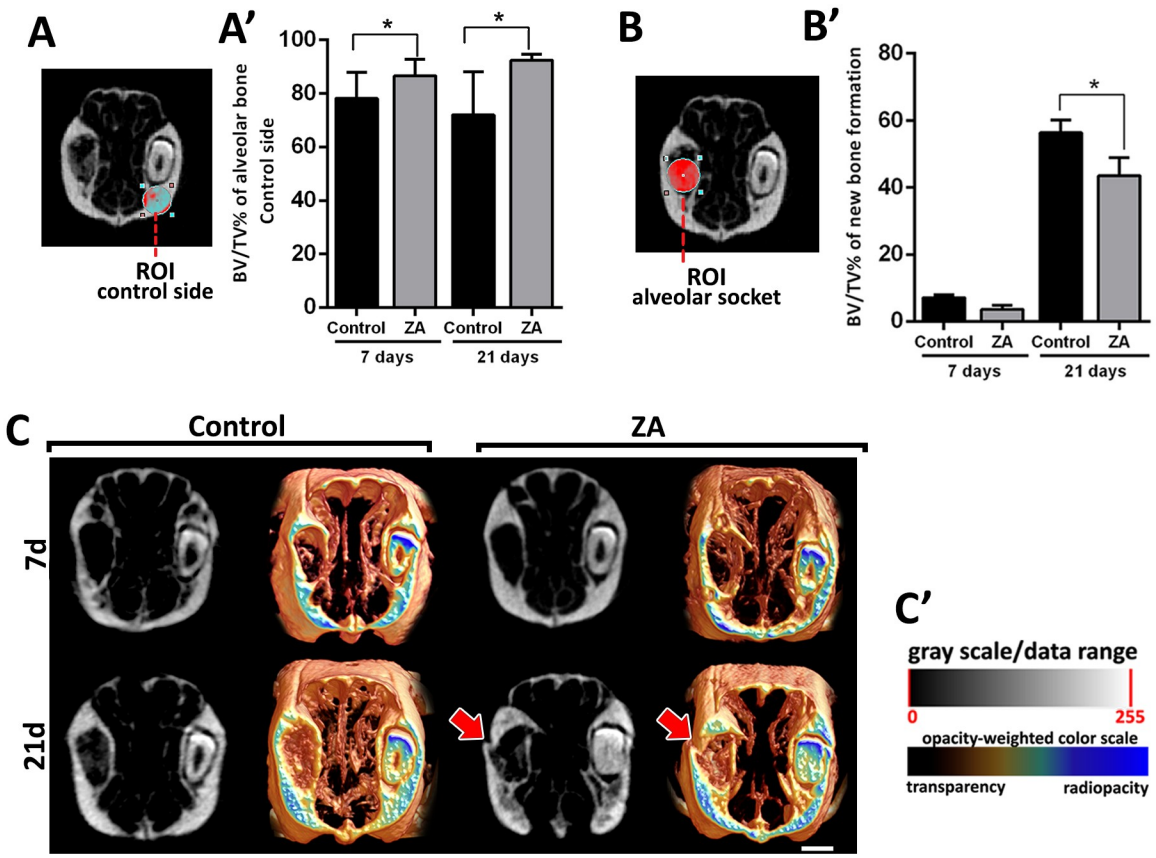

Fig 2. MicroCT evaluation of ZA cumulative effects on maxillary bone in NE sides and E sides (alveolar sockets post tooth extraction) in control and ZA treated mice. Senescent 129 Sv-WT female received IP injections of 0.9% saline solution (Vehicle) or 250 μg/Kg once a week, and upper right incisor were removed at 4 week of each treatment. Mice were euthanized for maxillary bones removal after 7days and 21days post tooth extraction. A) BV/TV (%) of intact bone (NE side) and B) in the alveolar socket post tooth extraction (E side). C)Three-dimensional representative images obtained with the CT-Vox software (Skyscan, Kontich, Belgium), showing transverse sections of Control and ZA maxillary bones at 7days and 21days post tooth extraction. A bone fracture is observed in ZA treated mouse at 21 days post tooth extraction (red arrow). Results are presented as the means (±SD) of each parameter. Symbol * indicates a statistically significant difference vs control ($p<0.05$).

https://doi.org/10.1371/journal.pone.0214173.g002

of healing (Control group) or MRONJ (ZA group) were evaluated for collagen fibers maturation, by the presence of birefringent collagen fibers (green, yellow and red) from the new bone or initial granulation tissue. While the Control group presented a gradual maturation of collagen fibers along 7 and 21 days, as well as a predominance of red spectrum fibers color at 21 days, the ZA group comparatively presented a lower quantity of collagen content at 7 days, and a predominance of green birefringent sprectrum collagen fibers at 21 days, indicating a disorganized organic matrix.

Histopathological and histomorphometric analysis

At day 7, dental sockets from the Control group healed without any complications, filled by a highly cellular and vascularized granulation tissue, when discrete osteogenesis was observed (Fig 4). After 21 days, mature bone trabeculae could be seen within a well-organized medulla. In the ZA group at day 7, a delay of healing process was indicated by the presence of focus of blood clot and its persistence until 21 days, as also confirmed by histomorphometry (Fig 4A and 4B). At day 21, intense leukocyte infiltration was observed, amongst thin primary

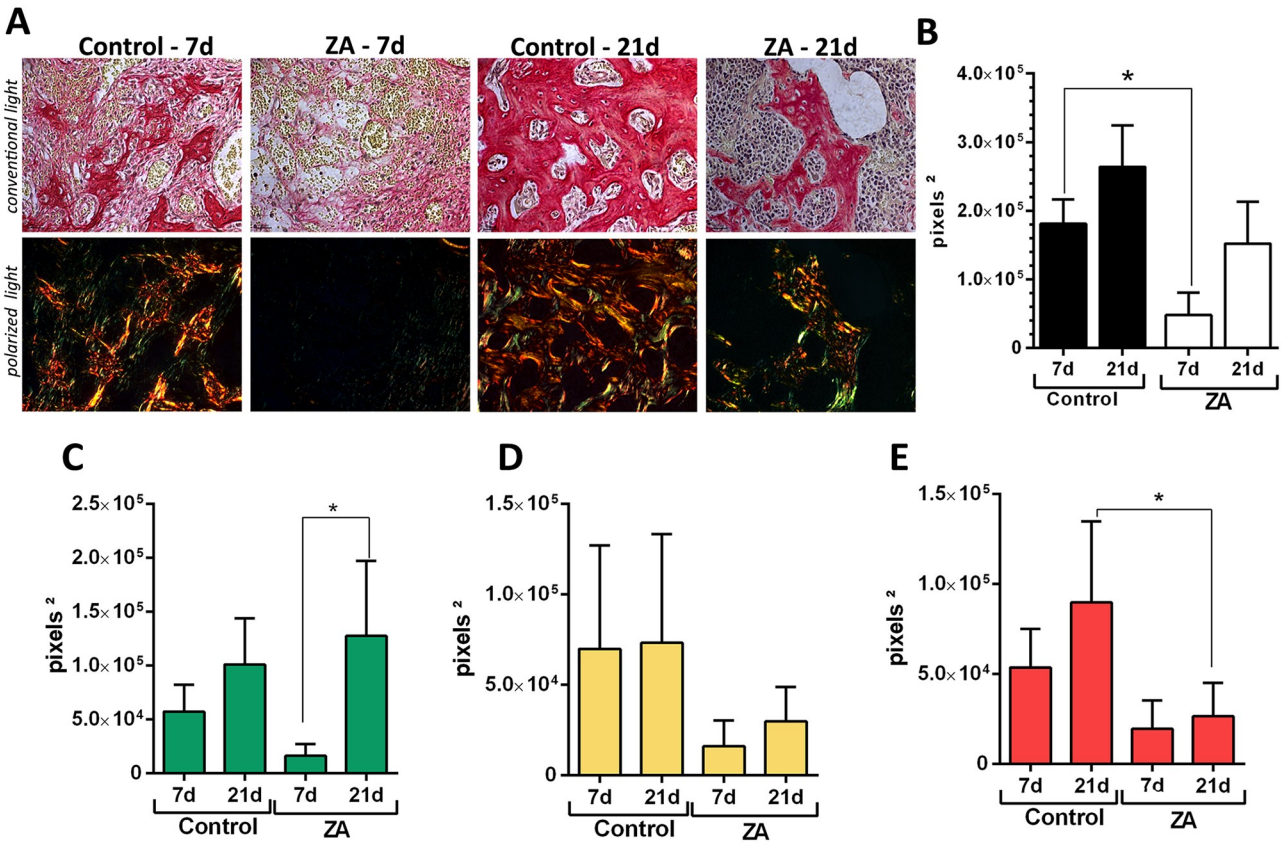

Fig 3. Birefringence analysis of collagen fibers in the alveolar sockets post tooth extraction (E sides) in control and ZA treated mice. Senescent 129 Sv-WT female mice received IP injections of 0.9% saline solution (Vehicle) or 250 μg/Kg once a week and upper right incisor were removed after 4 weeks of Vehicle or ZA treatments. Mice were euthanized for maxillary bones removal after 7days and 21days post tooth extraction. A)Representative transversal sections alveolar socket upon polarized and conventional light, to evaluate collagen fibers maturation in the different experimental groups and periods. As visualized upon polarized light, green birefringence color indicates thin fibers; yellow and red colors at birefringence analysis indicate thick collagen fibers. Original magnification was 40x. Intensity of birefringence measured from Image-analysis software (AxioVision, v. 4.8, CarlZeiss) to identify and quantify total area of collagen fibers (B) and area of collagen from each birefringence color (pixels^2) (C-green, D-yellow and E-red). Results are presented as mean and SD of pixels^2 for each color in the birefringence analysis. Symbol * indicates a statistically significant difference vs. control ($p<0.05$).

https://doi.org/10.1371/journal.pone.0214173.g003

trabeculae (Fig 4A and 4C). Also, areas of non-viable bone were noted, but interestingly serving as a scaffold for new bone formation in some areas (Fig 4A, 4D and 4E), along some discrete bone sequestrum. No biofilm formation was detected at this site of analysis for both the Control and ZA groups. In the ZA group, other findings were highlighted in the Fig 5, such as nodular formation of mineralized matrix surrounding blood clot, several detached osteoclasts in the connective tissue, short newly formed bone trabeculae and non-viable alveolar bone presenting empty lacunae of osteocytes close to the remaining periodontal ligament. Interestingly, the NE side (containing the left upper incisor), presented alveolar bone containing filled osteocytes lacunae in both Control and ZA groups (S2 Fig).

TRAP+ osteoclast staining analysis

Despite clear identification of some multinucleated OCs in the H&E stained sections, TRAP immunostaining was performed in alveolar sockets to accurately evaluate the area density (%) of OCs in the Control and ZA groups. TRAP+ OCs were found detached from bone, mainly in

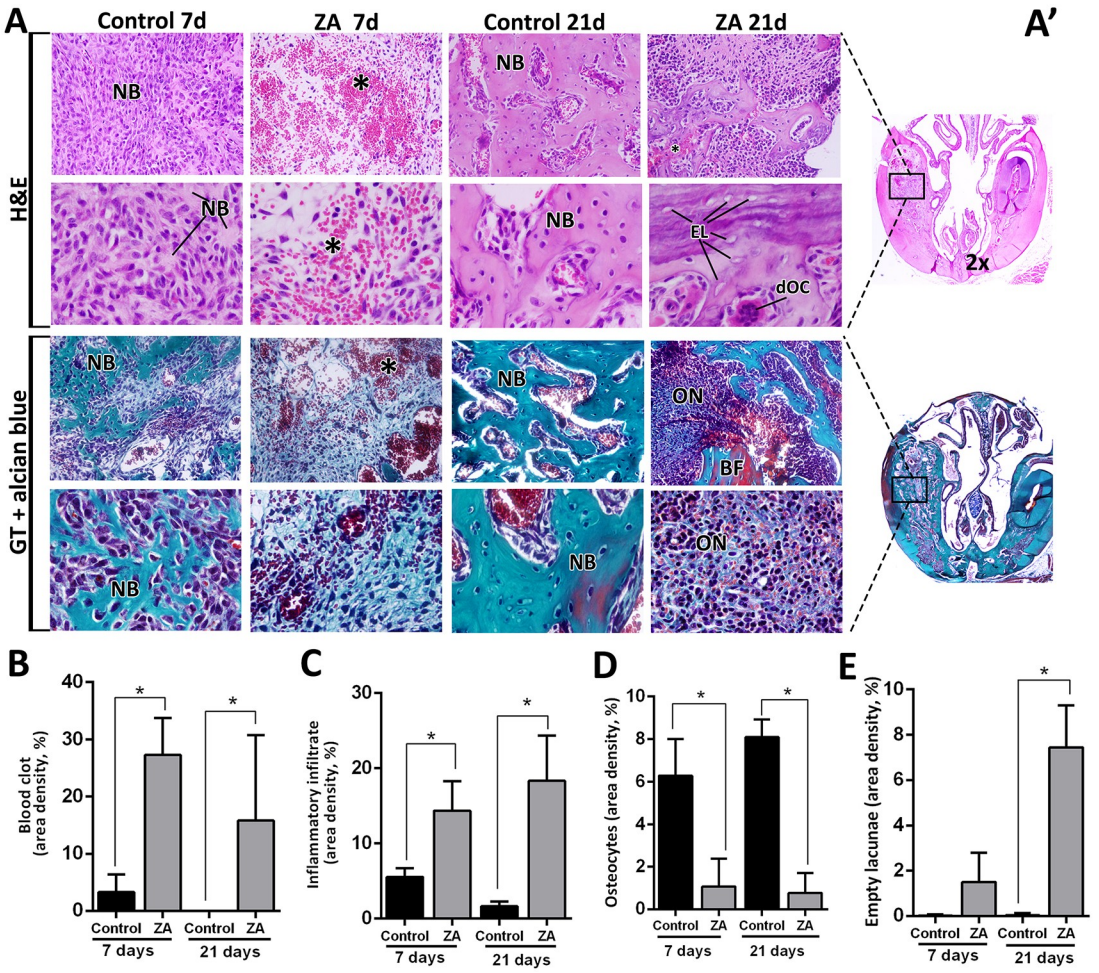

Fig 4. Histopathological and histomorphometric analysis of alveolar sockets post tooth extraction (E sides) in control and ZA treated mice. Senescent 129 Sv-WT female mice received IP injections of 0.9%saline solution(Vehicle) or 250 μg/Kg one a week and upper right incisor were removed after 4 weeks of Vehicle or ZA treatments. Mice were euthanized for maxillary bones removal after 7days and 21days post tooth extraction. A)Representative transversal sections are observed throughout days 7 and 21, from the central area of alveolar sockets (A'). Histological slides were stained with H&E (upper panel) and GT + Alcian blue (lower panel) and images were captured at 2x (entire section at left side) and 100x magnification (panels). Components of healing and MRONJ are indicated with letters and symbols, as follow: NB = new bone formation, ON = MRONJ sites with elevated inflammatory infiltrate, * = remaining/ non resorbed blood clot, BF = Bone fracture, EL = Empty Lacunae, dOC = detached OC. B-E) Histomorphometric analysis of healing or MRONJ parameters, including B) Remaining focus of blood clot, C) Inflammatory infiltrate, D) Osteocytes and E) Empty lacunae indicating non-viable bone. Results are presented as the means (±SD) of area density for each component. Symbol *indicate a statistically significant difference vs. control ($p<0.05$).

https://doi.org/10.1371/journal.pone.0214173.g004

the ZA group (1.60 ± 0.81) compared to the Control (0.016 ± 0.28) at 21 days, while the Control group had an increased quantity of attached TRAP+ OCs (6.40 ± 2.45) compared to the ZA group (1.93 ± 0.50) in this same time point. In total, TRAP+ OCs were significantly reduced in ZA group (3.53 ± 0.64) compared to Control (6.56 ± 2.17) at 21 days (Fig 6, Table 1).

TGF-β, Runx2, F4/80+ and PCNA+ cells

Other important factors involved in healing events were also evaluated by immunostaining (Fig 7A–7D and S3 Fig). An increased level of expression for TGF-β, Runx2 and F4/80+ cells was detected in the initial stages of healing (7days) in Control group (Fig 7A–7E). Comparatively with ZA, the area density (%) of TGF-β, Runx2 and F4/80+ cells were increased in the

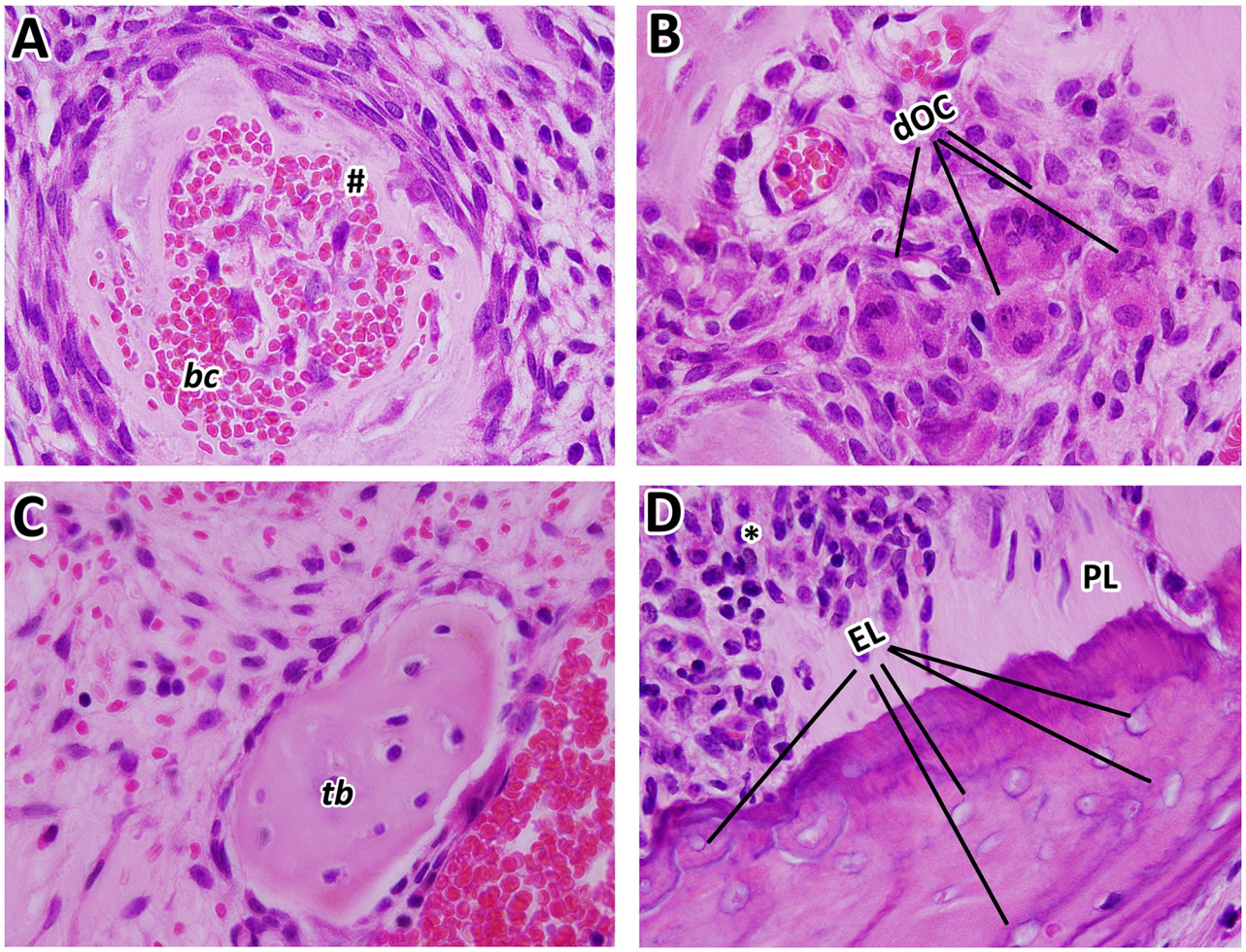

Fig 5. Details of MRONJ lesions in 129Sv senescent female mice treated with ZA at 21 days post tooth extraction. Representative transversal sections are observed throughout 21days, from the central area of alveolar sockets, 100x magnification. A) Nodular formation of mineralized matrix surrounding blood clot, associated with a highly cell contingent; B) detached osteoclast in the connective tissue; C) short newly formed bone trabeculae; D) non-vital alveolar bone presenting empty osteocytes lacunae close to the remaining periodontal ligament. MRONJ are indicated with letters and symbols, as follow: # nodular formation, dOC = detached OC, PL = remaining Periodontal Ligament, EL = Empty Lacunae, * = inflammatory infiltrate.

https://doi.org/10.1371/journal.pone.0214173.g005

Control considering the central area of alveolar sockets (Fig 7A–7D). Also, the immunolabeling for PCNA+ epithelial cells in the oral mucosa, showed an intense nuclear fluorescence in the Control group basal layers, while PCNA+ cells were scarcely found in the same regions of the ZA group (S3 Fig). At 21 days, Runx+2 cells were still found in increased number in the Control group compared to ZA. Mean and SD for all parameters are summarized in Table 1.

Discussion

This study investigated the bone healing after tooth extraction in senescent mice treated with zoledronic acid, as well as the usefulness of senescent 129/Sv female mice to understand the pathophysiology of MRONJ after tooth extraction. Previous MRONJ animal studies have not considered factors related to female human patients, such as age and post-menopause state, similar to what has been described in female human patients with risk factors for MRONJ [58]. Indeed, menopause female patients treated with nBPs are "10 fold higher risk to develop MRONJ at age 55 or older compared to young female patients" [1]. Matching the ages of

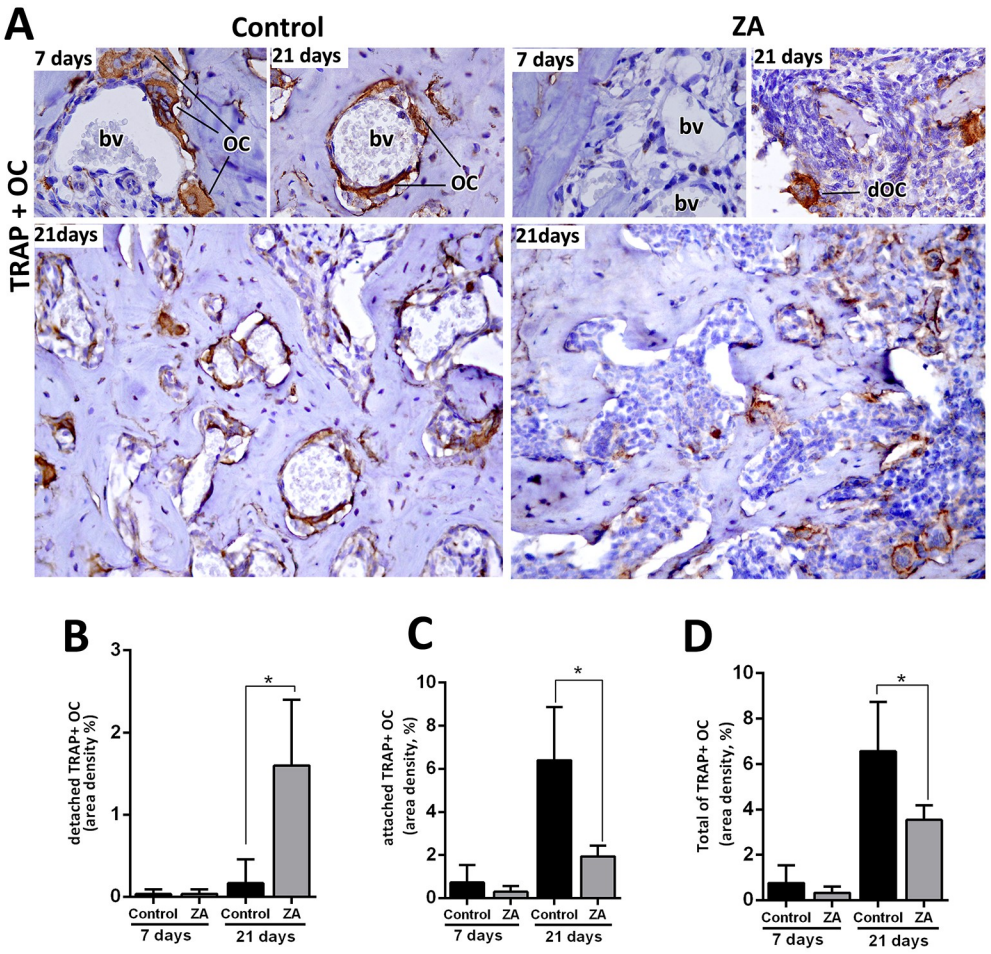

Fig 6. Immunolabeling and quantification of TRAP+OC in the control and ZA treated mice. Senescent 129 Sv-WT female mice received IP injections of 0.9% saline solution (Vehicle) or 250 μg/Kg one a week and upper right incisor were removed after 4 weeks of Vehicle or ZA treatments. Mice were euthanized for maxillary bones removal after 7days and 21days post tooth extraction. A) Representative transversal sections are observed throughout days 7 and 21, from the central area of alveolar sockets, for TRAP+OC in Control and ZA group. B-E) Quantitative and comparative analysis of detached TRAP+ OC (B), attached TRAP+ OC (C) and the Total of TRAP+OC considering the sum of detached and attached TRAP+ OC (D) in control vs ZA treated mice at days 7 and 21 post-extraction. Results are presented as the means (±SD) of area density (%). Symbol *indicate a statistically significant difference vs control ($p<0.05$). DAB chromogen and counterstaining with Harris' Hematoxylin.

https://doi.org/10.1371/journal.pone.0214173.g006

laboratory mice and humans, the correlated age for mice used in this study (64–68 weeks) is about 50–52 years in humans [21] and the senescent changes in mice begin in middle age, around 40–60 weeks [59]. The average age of menopause in women is around 51 years [60] which match the age in 129Sv females who were found in a persistent diestrum and in the post-menopausal period the at 64–68 weeks old (Fig 1A).

After demonstrating similar clinical preexisting conditions of MRONJ female patients in 129 Sv/female mice, MRONJ conditions were mimicked with upper right incisor extraction after 4 dosages of ZA or Vehicle (0.9% SS) (Fig 1B), and following a previous alveolar bone repair model in mice [52, 53]. The Control group female mice presented a gradual mineralized and organic matrix deposition and maturation along 7 and 21 days (Figs 2 and 3), compatible with other findings from 8 week-old C57Bl/6 WT mice alveolar sockets [52]. Also, histological features of bone healing and process of bone formation was gradual and consistent with other

Table 1. Summary of quantitative results for histomorphometry of area density (%).

Parameters/Groups	Control 7d	ZA 7d	Control 21d	ZA 21d
Blood clot	3.27±3.10	27.29±6.44*	0.00±0.00	15.79±14.96*
Inflam.Infiltrate	5.53±1.17	14.36±3.93*	1.62±0.62	18.33±6.03*
Osteocytes	6.57±2.06	1.63±1.32*	4.84±4.05	2.13±2.88*
Empty lacunae	0.02±0.05	0.75±0.95	0.04±0.08	7.43±7.85*
Detached TRAP+OC	0.03±0.05	0.04±0.05	0.016±0.28	1.60±0.81*
Attached TRAP+ OC	0.72±0.82	0.29±0.26	6.40±2.45	1.93±0.50*
Total of TRAP +OC	0.75±0.78	0.32±0.27	6.56±2.17	3.53±0.64*
TGFb+ cells	13.34±6.67	3.02±1.56*	4.16±1.58	5.79±0.40
Runx-2+ cells	10.71±1.63	1.32±1.41*	8.93±.76	2.75±1.36*
F4/80+ cells	6.01±3.16	1.90±1.71*	1.62±1.68	3.42±1.61

Results are presented as the means (±SD) for each parameter.

Symbol *indicate a statistically significant difference vs control at the same time point ($p<0.05$).

https://doi.org/10.1371/journal.pone.0214173.t001

findings in control groups of mice [52, 53] and rats [61, 62], making the vehicle group suitable for comparison with ZA treated mice.

While for humans there are established concept and classification for MRONJ [1, 58, 63], animal MRONJ models are not comparable in terms of diagnosis and can vary according to the protocol applied to trigger MRONJ (S1 Table). In humans, MRONJ is defined as an area of exposed bone in the oral cavity that does not heal within 8 weeks, in a patient who has been receiving or has been exposed to anti-resorptive (nBPs or denosumab) or anti-angiogenic therapy, and has not had radiation therapy in the craniofacial region [2, 58]. Although bone exposure is a part of diagnosis criteria, the current staging system proposed by the AAOMS [1, 63] includes a variant of MRONJ without bone exposure (stage 0), with no clinical evidence of necrotic bone and/or infection. In our study, only 40% of ZA group animals clinically presented delayed epithelial socket closure compared to the Control (S1 Fig) at 7 days, and a complete mucosal closure at 21 days. Additionally, no clinical suppuration and no biofilm evidences were noted in our model, because we do not use any periodontal pathogen inoculation. Indeed, laboratory mice (bred in ultra-hygienic environments) and human significantly differs in microbiota and pathogen-driven selection along their lives, which could reflect in different pattern of secondary infections in human and mice [20]. To address the oral bacterial influence on MRONJ pathogenesis, mice are inoculated with human periodontal pathogens in the local of oral injuries (e.g. *Fusobacterium nucleatum*) [26, 28].

In comparison to the available MRONJ mouse models (S1 Table), this study used a less traumatic triggering factor (tooth extraction of upper incisor instead of molars). Damage from extensive manipulation of bone, especially in advanced age conditions, does not reflect clinical conditions and could be a confounding factor for the healing process. In comparison with the present study, similar methodology was used in previous studies in rats (upper incisor extraction), in young (3 months old) [64] and senescent animals (20 months old) [62], where animals not necessarily developed clinical findings of MRONJ lesions, but all of them revealed histological features of this pathological conditions [64]. Despite of the differences in animal clinical findings with other studies [62, 64], 100% of our ZA samples presented delayed mineralized and organic bone matrix deposition, and also decreased level of collagen maturation along 7 and 21 days (Figs 2 and 3). These findings are consistent with those in other studies using senescent female rats treated with ZA [61]. Col1a1 is significantly downregulated in MRONJ lesions in mice, affecting the collagen deposition, mainly by inhibition of TGF-β signaling

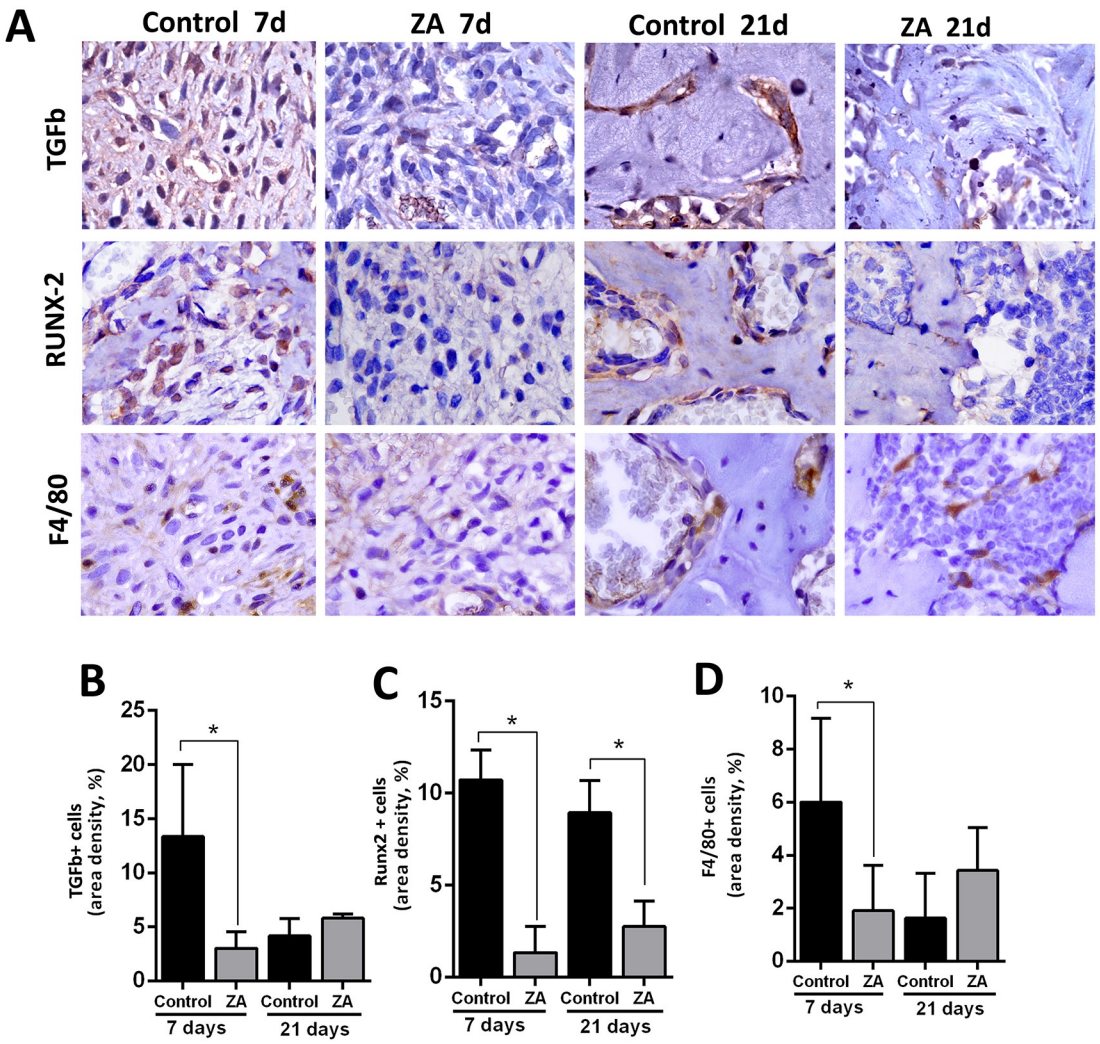

Fig 7. Immunolabeling and counting of TGFb, Runx-2 and F480+ cells of alveolar sockets post tooth extraction in control and ZA treated mice. Senile 129 Sv-WT female mice received IP injections of 0.9% saline solution (Vehicle) or 250 μg/Kg one a week and upper right incisor were removed after 4 weeks of Vehicle or ZA treatments. Mice were euthanized for maxillary bones removal after 7days and 21days post tooth extraction. A) Representative transversal sections are observed throughout days 7 and 21, from the central area of alveolar sockets, for TGFb, Runx2 and F4/80+ cells (B-D) Quantitative and comparative analysis TGFb+cells (B), Runx-2+ cells (C) and F4/80+ cells (D) in Control vs ZA treated mice at days 7 and 21 post-extraction. Results are presented as the means (±SD) of area density (%). Symbol *indicate a statistically significant difference vs. control ($p<0.05$). DAB chromogen and counterstaining with Harris' Hematoxylin.

https://doi.org/10.1371/journal.pone.0214173.g007

pathway [23]. In our histopathological analysis, 100% of our ZA treated mice presented a delayed bone healing and MRONJ lesions histological characteristics (Figs 4 and 5). These compare with other findings in mice [23, 39], rats [61, 62, 64] and humans [12, 13], including intense leukocyte infiltration, areas of non-vital bone and discrete bone sequestrum.

To accurately analyze the effect of ZA administration on bone cells, we investigated the morphological and histomorphometric changes in osteocytes and empty lacunae (Fig 3D and 3E) as well as TRAP+ OC's (Fig 6). As expected, ZA group presented a decreased number of Total TRAP+ OC's compared to the Control, as observed in other animal models [61] and humans [65]. The majority of TRAP+ OC's in ZA samples were detached from the bone matrix which resembled MRONJ characteristics in senescent rats [62] and human biopsies

[65]. Additionally, an increased quantity of empty lacunae was found in the ZA E site compared to Control E site (Fig 4). Empty lacunae is one diagnostic factor for osteonecrosis [12, 13] and is consistent with other findings in mice MRONJ lesions [23]. Interestingly, the greatest amount of empty lacunae was found at E sites, but not in the NE sites in ZA-treated mice (S2 Fig). This finding highlights a hindrance to bone repair processes in which, under normal circumstances, osteocytes undergo apoptosis and recruit osteoclasts to resorb damaged bone [66]. Furthermore, it emphasizes that trauma is crucial for osteocyte apoptosis, which is a hallmark characteristic of necrotic bone [12, 13].

Both osteoclast and osteocyte biology may assist in understanding the pathogenesis of MRONJ, partially because of the osteocyte signaling to osteoclasts in injury and under mechanical loading conditions [66]. At the ultrastructural level, nBP's target OC's by blocking the mevalonate pathway, thereby negatively interferes with the organization of their cytoskeleton, thus blocking the formation of the ruffled border [67]. The cell resorption compartment, where the protons and proteolytic enzymes are released for the dissolution of bone mineral and organic contends, cannot be formed leading to apoptosis of OCs [47].

While nBP's induce OC apoptosis, some evidence has revealed an opposite effect on the osteocytes, which is a required effect for blocking bone loss in osteoporotic long bones [68, 69]. However, osteocyte apoptosis is essential to replace damaged bone [68]. In aged bone, senescent osteocytes will actually increase their number of dendritic processes [70], indicating increases in regulation of bone homeostasis. When osteocytes age, some of these cells die, though in areas of low bone turnover, such as ear bones, empty lacunae do not necessarily indicate necrotic bone [71, 72].

One important function of osteocytes is to sense mechanical pressure on bone and send signals to resorb bone where deemed appropriate [73–75]. A previous study by Marx in 2014 reported that the incidence of MRONJ in the oral cavity is highest in areas of high mechanical load on bone (posterior mandibular lingual cortex, edentulous alveolar ridge covered by dentures, and the lamina dura) [73]. Marx also reported that mechanical loading of bone causes decreased osteocyte OPG secretion, thus an increased RANKL/OPG ratio and increased osteoclast recruitment to resorb the involved bone [73]. Furthermore, excessive or insufficient levels of mechanical loading cause apoptosis of osteocytes and induction of osteoclastic bone resorption [74–76]. If this bone is nBP-laden, these resorbing osteoclasts would undergo apoptosis and leave the remaining bone with its empty lacunae. When tooth extraction causes bony injury to the alveolar socket, the healing process is similar to aforementioned bone resorption. Most osteocytes more than 1–2 mm from a bone fracture do not die [75] and will increase RANKL and decrease OPG production [77]. Concurrently, osteocytes within 1–2 mm of the fracture site undergo apoptosis and release RANKL-wielding vesicles that promote osteoclast recruitment [78]. Osteocyte apoptosis in damaged bone therefore leaves an acellular bone matrix ready to be resorbed by recruited osteoclasts [75]. The MRONJ phenotype results in part from the detachment and death of recruited osteoclasts when they ingest nBP-laden bone. Furthermore, the bone matrix has empty osteocyte lacunae from the initial response to the trauma, as observed in the injured socket areas in this study (S2 and S3 Figs).

Our data has demonstrated a decreased number of TGF-β+ cells and Runx-2+ cells (committed osteoblasts) in ZA treated mice, as similarly observed in other MRONJ mice [23] and rat models [62], respectively. TGF-ß1 signaling pathway is necessary to activate the transcription factor Runx-2 (a global regulator of osteogenesis) and both are significantly up-regulated in control conditions along alveolar bone repair in mice, concomitant with new bone differentiation and bone deposition [52, 53]. In this context, another important effect of nBP's is on new bone cells' differentiation in injured sites, since TGF-β1 signaling pathway is also significantly suppressed in MRONJ lesions at the clinical level [79].

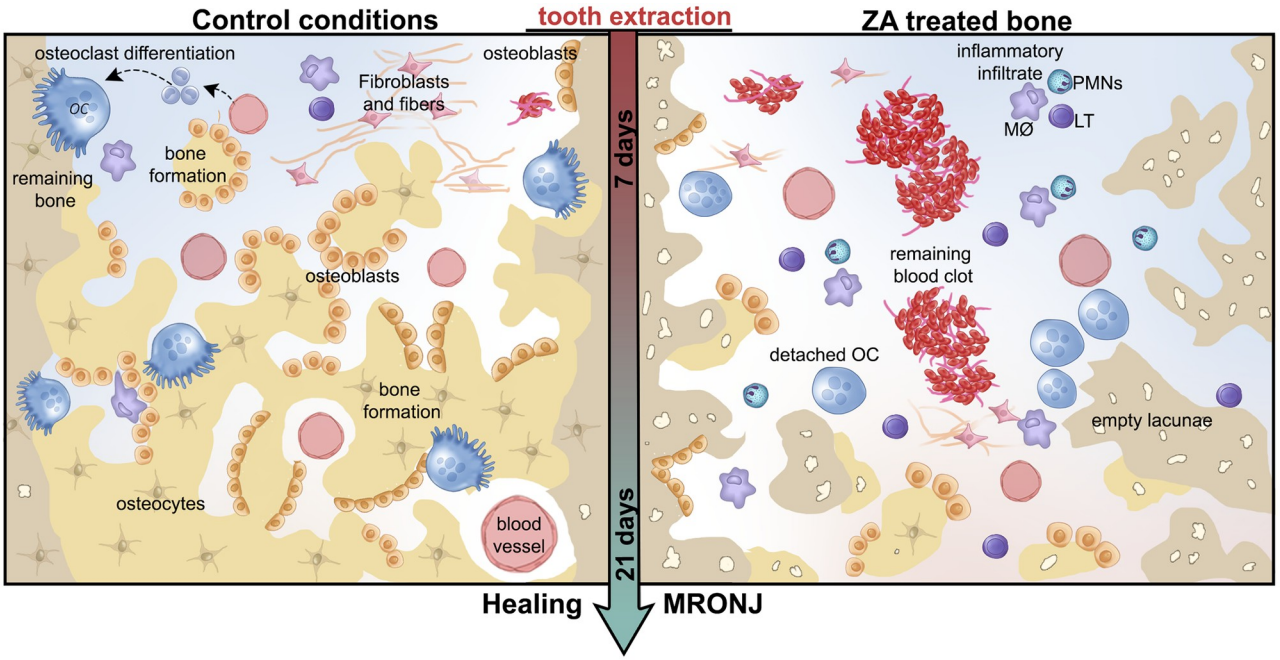

Fig 8. Graphical representation of microscopic events during initial and late time points post tooth extraction in control conditions compared to MRONJ model in senescent 129 Sv WT female mice. In summary, senescent 129 Sv female mice treated with cumulative dosages of Zoledronic acid present a disrupted healing process post tooth extraction compared to Control conditions. While bone formation and remodeling occurs along 21 days in control conditions, in the MRONJ phenotype, a delayed blood clot and debris removal, increased inflammatory infiltration, increased occurrence of empty lacunae and bone sequestrum, detached osteoclasts are seen until the later time points of 21 days.

https://doi.org/10.1371/journal.pone.0214173.g008

Finally, although nBP influence on bone cells has been previously demonstrated, its action on immune cells remains largely unclear. Several studies have revealed that monocytes and macrophages are capable of internalizing nBP's [67, 80]. Post-tooth extraction experimental models performed in mice revealed a high polarization of M1 macrophages induced by IL-17 increase in non-healing sockets. This evidence demonstrates an imbalance in M1/M2 ratio, which is related to the pathogenesis of disease [17]. In this study, a decreased migration of F4/80+ cells at 7 days was observed in ZA mice compared to the Control, while a slight increase in migration was observed at 21 days in MRONJ lesions (Fig 7E). Accordingly, a delayed removal of blood clot and an increased persistence of general inflammatory infiltration were also noted in ZA group compared to the Control (Fig 3B and 3C). F4/80+ cells are supposed to be mainly macrophages, as has been demonstrated in similar tooth extraction mouse model [53]. In this context, macrophages are supposed to be important for producing growth factors, activation of immune response and clearance of tissue debris, blood clot and necrotic cells [53]. According to these findings, this study also draws the attention for future evaluations of interferences on immunological system caused by the nBPs.

Conclusions

In summary, despite the limitations of this study, the presented findings are consistent with the accepted MRONJ phenotype, that include delayed blood clot and debris removal, increased and disruption of inflammatory infiltration, increased occurrence of empty lacunae and bone sequestrum in injured alveolar socket, fewer TRAP+ OCs, and potential inhibition of bone-related growth factors accompanied by delayed bone matrix formation and maturation (Fig 8). Considering all these observations and comparing with previous descriptions of MRONJ in

humans, this MRONJ mouse model offers a novel experimental tool for development of future pre-clinical interventions.

Supporting information

S1 Table. Summary of MRONJ mice models.
(DOC)

S1 Fig. Macroscopical view of MRONJ model in senescent female 129 Sv mice. A) At 68 weeks of age, mice were subjected to atraumatically extraction of right upper incisor. B) Macroscopical occlusal views present clinical aspect of healing oral mucosal post-tooth extraction, 100% of control mice had a complete mucosal closure at 7d and 21 days, while 40% of ZA treated mice presented delayed in epithelial socket closure at 7 days (dotted line), but a complete mucosal closure at 21 days.
(TIF)

S2 Fig. Representative transversal sections from alveolar bone of extraction sites (1–4) and control sites (5–8) in control and ZA group at 7 days post tooth extraction. A) Control group extraction sites (A1-A4) and Control sites (A5-A8) filled with osteocytes (black arrows). B) ZA group extraction sites (A1-A4) present several empty lacunae (red arrows), while Control sites (A5-A8) remain filled with osteocytes (black arrows). Histological slides were stained with H&E (upper panel) and GT+Alcian blue (lower panel) and images were captured at 2x (entire section at left side) and 100x magnification (panels).
(TIF)

S3 Fig. Immunolabeling for PCNA+ epithelial cells from the alveolar socket area at 7days post tooth extraction in senescent 129 Sv-WT female. Mice received IP injections of 0.9% saline solution (Vehicle) or 250 μg/Kg one a week and upper right incisor were removed after 4 weeks of Vehicle or ZA treatments. Mice were euthanized for maxillary bones removal after 7days post tooth extraction. Secondary antibody Cy3 (#715-165-150, Jackson ImmunoResearch Laboratories, West Grove, PA, USA) for detection of PCNA and DAPI (D9542-50, Sigma-Aldrich Corp., St. Louis, MO, USA) for nuclear staining.
(TIF)

Acknowledgments

The authors acknowledge Ms. Maira Cristina Couto for her excellent technical assistance in this study.

Author Contributions

Conceptualization: Claudia Cristina Biguetti, Edilson Ervolino, Walid D. Fakhouri, Mariza Akemi Matsumoto.

Data curation: Claudia Cristina Biguetti, André Hergesel De Oliva, Kent Healy, Ramez Hassan Mahmoud, Isabela Do Carmo Custódio, Dulce Helena Constantino, Edilson Ervolino, Marco Antonio Hungaro Duarte, Mariza Akemi Matsumoto.

Formal analysis: Claudia Cristina Biguetti, André Hergesel De Oliva, Kent Healy, Ramez Hassan Mahmoud, Isabela Do Carmo Custódio, Dulce Helena Constantino, Edilson Ervolino, Marco Antonio Hungaro Duarte, Walid D. Fakhouri, Mariza Akemi Matsumoto.

Funding acquisition: Mariza Akemi Matsumoto.

Investigation: Claudia Cristina Biguetti, André Hergesel De Oliva, Kent Healy, Ramez Hassan Mahmoud, Isabela Do Carmo Custódio, Dulce Helena Constantino, Marco Antonio Hungaro Duarte, Walid D. Fakhouri, Mariza Akemi Matsumoto.

Methodology: Claudia Cristina Biguetti, André Hergesel De Oliva, Kent Healy, Ramez Hassan Mahmoud, Isabela Do Carmo Custódio, Dulce Helena Constantino, Marco Antonio Hungaro Duarte, Walid D. Fakhouri, Mariza Akemi Matsumoto.

Project administration: Claudia Cristina Biguetti, Mariza Akemi Matsumoto.

Resources: Dulce Helena Constantino, Edilson Ervolino, Marco Antonio Hungaro Duarte, Mariza Akemi Matsumoto.

Software: Claudia Cristina Biguetti.

Supervision: Edilson Ervolino, Walid D. Fakhouri, Mariza Akemi Matsumoto.

Validation: Claudia Cristina Biguetti, Ramez Hassan Mahmoud, Edilson Ervolino, Marco Antonio Hungaro Duarte, Walid D. Fakhouri.

Visualization: Claudia Cristina Biguetti, André Hergesel De Oliva, Kent Healy, Ramez Hassan Mahmoud, Isabela Do Carmo Custódio, Dulce Helena Constantino, Edilson Ervolino, Walid D. Fakhouri.

Writing – original draft: Claudia Cristina Biguetti, André Hergesel De Oliva, Kent Healy, Ramez Hassan Mahmoud, Isabela Do Carmo Custódio, Dulce Helena Constantino, Edilson Ervolino, Walid D. Fakhouri.

Writing – review & editing: Claudia Cristina Biguetti, Walid D. Fakhouri, Mariza Akemi Matsumoto.

References

1. Ruggiero SL, Dodson TB, Fantasia J, Goodday R, Aghaloo T, Mehrotra B, et al. American Association of Oral and Maxillofacial Surgeons position paper on medication-related osteonecrosis of the jaw-2014 update. J Oral Maxillofac Surg 2014. 72(10): p. 1938–56. https://doi.org/10.1016/j.joms.2014.04.031 PMID: 25234529
2. Khan AA, Morrison A, Kendler DL, Rizzoli R, Hanley DA, Felsenberg D, et al. Case-Based Review of Osteonecrosis of the Jaw (ONJ) and Application of the International Recommendations for Management From the International Task Force on ONJ. J Clin Densitom 2017. 20(1): p. 8–24. https://doi.org/10.1016/j.jocd.2016.09.005 PMID: 27956123
3. Schwartz HC. American Association of Oral and Maxillofacial Surgeons position paper on medication-related osteonecrosis of the jaw-2014 update and CTX. J Oral Maxillofac Surg, 2015. 73(3): p. 377.
4. Mavrokokki T, Cheng A, Stein B, Goss A. Nature and frequency of bisphosphonate-associated osteonecrosis of the jaws in Australia. J Oral Maxillofac Surg, 2007. 65(3): p. 415–23. https://doi.org/10.1016/j.joms.2006.10.061 PMID: 17307586
5. Yarom N, Yahalom R, Shoshani Y, Hamed W, Regev E, Elad S. Osteonecrosis of the jaw induced by orally administered bisphosphonates: incidence, clinical features, predisposing factors and treatment outcome. Osteoporos Int, 2007. 18(10): p. 1363–70. https://doi.org/10.1007/s00198-007-0384-2 PMID: 17598065
6. Kwon YD, Ohe JY, Kim DY, Chung DJ, Park YD. Retrospective study of two biochemical markers for the risk assessment of oral bisphosphonate-related osteonecrosis of the jaws: can they be utilized as risk markers? Clin Oral Implants Res, 2011. 22(1): p. 100–5. https://doi.org/10.1111/j.1600-0501.2010.01965.x PMID: 20946206
7. Hoff AO, Toth BB, Altundag K, Johnson MM, Warneke CL, Hu M, et al. Frequency and risk factors associated with osteonecrosis of the jaw in cancer patients treated with intravenous bisphosphonates. J Bone Miner Res, 2008. 23(6): p. 826–36. https://doi.org/10.1359/jbmr.080205 PMID: 18558816
8. Berenson JR, Vescio R, Henick K, Nishikubo C, Rettig M, Swift RA, et al. A Phase I, open label, dose ranging trial of intravenous bolus zoledronic acid, a novel bisphosphonate, in cancer patients with metastatic bone disease. Cancer, 2001. 91(1): p. 144–54. PMID: 11148571

9. Van Poznak CH, Temin S, Yee GC, Janjan NA, Barlow WE, Biermann JS, et al. American Society of Clinical Oncology executive summary of the clinical practice guideline update on the role of bone-modifying agents in metastatic breast cancer. J Clin Oncol, 2011. 29(9): p. 1221–7. https://doi.org/10.1200/JCO.2010.32.5209 PMID: 21343561
10. Hamdy RC. Zoledronic acid: clinical utility and patient considerations in osteoporosis and low bone mass. Drug Des Devel Ther, 2010. 4: p. 321–35. https://doi.org/10.2147/DDDT.S6287 PMID: 21151620
11. Lambrinoudaki I, Vlachou S, Galapi F, Papadimitriou D, Papadias K. Once-yearly zoledronic acid in the prevention of osteoporotic bone fractures in postmenopausal women. Clin Interv Aging, 2008. 3(3): p. 445–51. PMID: 18982915
12. Marx RE, Tursun R. Suppurative osteomyelitis, bisphosphonate induced osteonecrosis, osteoradionecrosis: a blinded histopathologic comparison and its implications for the mechanism of each disease. Int J Oral Maxillofac Surg, 2012. 41(3): p. 283–9. https://doi.org/10.1016/j.ijom.2011.12.016 PMID: 22244079
13. De Antoni CC, Matsumoto MM, Silva AA, Curi MM, Santiago JF Jr, Sassi LM, et al. Medication-related osteonecrosis of the jaw, osteoradionecrosis, and osteomyelitis: A comparative histopathological study. Braz Oral Res, 2018. 32: p. e23. https://doi.org/10.1590/1807-3107bor-2018.vol32.0023 PMID: 29723337
14. Vermeer J, Renders G, van Duin MA, Jansen I, Bakker LF, Kroon SA, et al. Bone-site-specific responses to zoledronic acid. Oral Dis, 2017. 23(1): p. 126–133. https://doi.org/10.1111/odi.12587 PMID: 27706930
15. Akita Y, Kuroshima S, Nakajima K, Hayano H, Kanai R, Sasaki M, et al. Effect of anti-angiogenesis induced by chemotherapeutic monotherapy, chemotherapeutic/bisphosphonate combination therapy and anti-VEGFA mAb therapy on tooth extraction socket healing in mice. J Bone Miner Metab, 2018. 36(5): p. 547–559. https://doi.org/10.1007/s00774-017-0872-1 PMID: 29043461
16. Gao SY, Zheng GS, Wang L, Liang YJ, Zhang SE, Lao XM, et al. Zoledronate suppressed angiogenesis and osteogenesis by inhibiting osteoclasts formation and secretion of PDGF-BB. PLoS One, 2017. 12 (6): p. e0179248. https://doi.org/10.1371/journal.pone.0179248 PMID: 28594896
17. Zhang Q, Atsuta I, Liu S, Chen C, Shi S, Shi S, et al. IL-17-mediated M1/M2 macrophage alteration contributes to pathogenesis of bisphosphonate-related osteonecrosis of the jaws. Clin Cancer Res, 2013. 19(12): p. 3176–88. https://doi.org/10.1158/1078-0432.CCR-13-0042 PMID: 23616636
18. de Barros Silva PG, de Oliveira CC, Brizeno L, Wong D, Lima Júnior R, Gonçalves RP, et al. Immune cellular profile of bisphosphonate-related osteonecrosis of the jaw. Oral Dis, 2016. 22(7): p. 649–57. https://doi.org/10.1111/odi.12513 PMID: 27232600
19. Hoefert S, Schmitz I, Weichert F, Gaspar M, Eufinger H. Macrophages and bisphosphonate-related osteonecrosis of the jaw (BRONJ): evidence of local immunosuppression of macrophages in contrast to other infectious jaw diseases. Clin Oral Investig, 2015. 19(2): p. 497–508. https://doi.org/10.1007/s00784-014-1273-7 PMID: 24957986
20. Tao L, Reese TA. Making Mouse Models That Reflect Human Immune Responses. Trends Immunol, 2017. 38(3): p. 181–193. https://doi.org/10.1016/j.it.2016.12.007 PMID: 28161189
21. Dutta S, Sengupta P. Men and mice: Relating their ages. Life Sci, 2016. 152: p. 244–8. https://doi.org/10.1016/j.lfs.2015.10.025 PMID: 26596563
22. Biguetti CC, Cavalla F, Silveira EM, Fonseca AC, Vieira AE, Tabanez AP, et al. Oral implant osseointegration model in C57Bl/6 mice: microtomographic, histological, histomorphometric and molecular characterization. Journal of Applied Oral Science, 2018: p. 1–24.
23. Kim S, Williams DW, Lee C, Kim T, Arai A, Shi S, et al. IL-36 Induces Bisphosphonate-Related Osteonecrosis of the Jaw-Like Lesions in Mice by Inhibiting TGF-beta-Mediated Collagen Expression. J Bone Miner Res, 2017. 32(2): p. 309–318. https://doi.org/10.1002/jbmr.2985 PMID: 27567012
24. Kim T, Kim S, Song M, Lee C, Yagita H, Williams DW, et al. Removal of Pre-Existing Periodontal Inflammatory Condition before Tooth Extraction Ameliorates Medication-Related Osteonecrosis of the Jaw-Like Lesion in Mice. Am J Pathol, 2018. 188(10): p. 2318–2327. https://doi.org/10.1016/j.ajpath.2018.06.019 PMID: 30059656
25. Kuroshima S, Sasaki M, Nakajima K, Tamaki S, Hayano H, Sawase T. Transplantation of noncultured Stromal Vascular Fraction Cells of Adipose Tissue Ameliorates Osteonecrosis of the Jaw-Like Lesions in Mice. J Bone Miner Res, 2018. 33(1): p. 154–166. https://doi.org/10.1002/jbmr.3292 PMID: 28902422
26. Movila A, Mawardi H, Nishimura K, Kiyama T, Egashira K, Kim JY, et al. Possible pathogenic engagement of soluble Semaphorin 4D produced by gamma deltaT cells in medication-related osteonecrosis of the jaw (MRONJ). Biochem Biophys Res Commun, 2016. 480(1): p. 42–47. https://doi.org/10.1016/j.bbrc.2016.10.012 PMID: 27720716

27. Sun Y, Kaur K, Kanayama K, Morinaga K, Park S, Hokugo A, et al. Plasticity of Myeloid Cells during Oral Barrier Wound Healing and the Development of Bisphosphonate-related Osteonecrosis of the Jaw. J Biol Chem, 2016. 291(39): p. 20602–16. https://doi.org/10.1074/jbc.M116.735795 PMID: 27514746

28. Mawardi H, Giro G, Kajiya M, Ohta K, Almazrooa S, Alshwaimi E. A role of oral bacteria in bisphosphonate-induced osteonecrosis of the jaw. J Dent Res, 2011. 90(11): p. 1339–45. https://doi.org/10.1177/0022034511420430 PMID: 21921248

29. Matsuura Y, Atsuta I, Ayukawa Y, Yamaza T, Kondo R, Takahashi A, et al. Therapeutic interactions between mesenchymal stem cells for healing medication-related osteonecrosis of the jaw. Stem Cell Res Ther, 2016. 7(1): p. 119. https://doi.org/10.1186/s13287-016-0367-3 PMID: 27530108

30. Soundia A, Hadaya D, Esfandi N, de Molon RS, Bezouglaia O, Dry SM, et al. Osteonecrosis of the jaws (ONJ) in mice after extraction of teeth with periradicular disease. Bone, 2016. 90: p. 133–41. https://doi.org/10.1016/j.bone.2016.06.011 PMID: 27327410

31. Song M, Alshaikh A, Kim T, Kim S, Dang M, Mehrazarin S et al. Preexisting Periapical Inflammatory Condition Exacerbates Tooth Extraction-induced Bisphosphonate-related Osteonecrosis of the Jaw Lesions in Mice. J Endod, 2016. 42(11): p. 1641–1646. https://doi.org/10.1016/j.joen.2016.07.020 PMID: 27637460

32. Kikuiri T, Kim I, Yamaza T, Akiyama K, Zhang Q, Li Y, et al. Cell-based immunotherapy with mesenchymal stem cells cures bisphosphonate-related osteonecrosis of the jaw-like disease in mice. J Bone Miner Res, 2010. 25(7): p. 1668–79. https://doi.org/10.1002/jbmr.37 PMID: 20200952

33. Bi Y, Gao Y, Ehirchiou D, Cao C, Kikuiri T, Le A, et al. Bisphosphonates cause osteonecrosis of the jaw-like disease in mice. Am J Pathol, 2010. 177(1): p. 280–90. https://doi.org/10.2353/ajpath.2010.090592 PMID: 20472893

34. Su J, Feng M, Han W, Zhao H. The effects of bisphosphonate on the remodeling of different irregular bones in mice. J Oral Pathol Med, 2015. 44(8): p. 638–48. https://doi.org/10.1111/jop.12281 PMID: 25370709

35. Zhao Y, Wang L, Liu Y, Akiyama K, Chen C, Atsuta I, et al. Technetium-99 conjugated with methylene diphosphonate ameliorates ovariectomy-induced osteoporotic phenotype without causing osteonecrosis in the jaw. Calcif Tissue Int, 2012. 91(6): p. 400–8. https://doi.org/10.1007/s00223-012-9649-7 PMID: 23064899

36. Kang B, Cheong S, Chaichanasakul T, Bezouglaia O, Atti E, Dry SM, et al. Periapical disease and bisphosphonates induce osteonecrosis of the jaws in mice. J Bone Miner Res, 2013. 28(7): p. 1631–40. https://doi.org/10.1002/jbmr.1894 PMID: 23426919

37. Park S, Kanayama K, Kaur K, Tseng HH, Banankhah S, Quje DT, et al. Osteonecrosis of the Jaw Developed in Mice: Disease variants regulated by Gammadelta T Cells in oral mucosal barrier immunity. J Biol Chem, 2015. 290(28): p. 17349–66. https://doi.org/10.1074/jbc.M115.652305 PMID: 26013832

38. Aghaloo TL, Cheong S, Bezouglaia O, Kostenuik P, Atti E, Dry SM, et al. RANKL inhibitors induce osteonecrosis of the jaw in mice with periapical disease. J Bone Miner Res, 2014. 29(4): p. 843–54. https://doi.org/10.1002/jbmr.2097 PMID: 24115073

39. de Molon RS, Cheong S, Bezouglaia O, Dry SM, Pirih F, Cirelli JA, et al. Spontaneous osteonecrosis of the jaws in the maxilla of mice on antiresorptive treatment: a novel ONJ mouse model. Bone, 2014. 68: p. 11–9. https://doi.org/10.1016/j.bone.2014.07.027 PMID: 25093262

40. Mekada K, Abe K, Murakami A, Nakamura S, Nakata H, Moriwaki K, et al. Genetic differences among C57BL/6 substrains. Exp Anim, 2009. 58(2): p. 141–9. PMID: 19448337

41. Sabsovich I, Clark JD, Liao G, Peltz G, Lindsey DP, Jacobs CR, et al. Bone microstructure and its associated genetic variability in 12 inbred mouse strains: microCT study and in silico genome scan. Bone, 2008. 42(2): p. 439–51. https://doi.org/10.1016/j.bone.2007.09.041 PMID: 17967568

42. de Molon RS, Hsu C, Bezouglaia O, Dry SM, Pirih FQ, Soundia A, et al. Rheumatoid Arthritis Exacerbates the Severity of Osteonecrosis of the Jaws (ONJ) in Mice. A Randomized, Prospective, Controlled Animal Study. J Bone Miner Res, 2016. 31(8): p. 1596–607. https://doi.org/10.1002/jbmr.2827 PMID: 26950411

43. de Molon RS, Shimamoto H, Bezouglaia O, Pirih FQ, Dry SM, Kostenuik P, et al. OPG-Fc but Not Zoledronic Acid Discontinuation Reverses Osteonecrosis of the Jaws (ONJ) in Mice. J Bone Miner Res, 2015. 30(9): p. 1627–40. https://doi.org/10.1002/jbmr.2490 PMID: 25727550

44. Córdova LA, Guilbaud F, Amiaud J, Battaglia S, Charrier C, Lezot F, et al. Severe compromise of preosteoblasts in a surgical mouse model of bisphosphonate-associated osteonecrosis of the jaw. J Craniomaxillofac Surg, 2016. 44(9): p. 1387–94. https://doi.org/10.1016/j.jcms.2016.07.015 PMID: 27519659

45. Williams DW, Lee C, Kim T, Yagita H, Wu H, Park S, et al. Impaired bone resorption and woven bone formation are associated with development of osteonecrosis of the jaw-like lesions by bisphosphonate

and anti-receptor activator of NF-kappaB ligand antibody in mice. Am J Pathol, 2014. 184(11): p. 3084–93. https://doi.org/10.1016/j.ajpath.2014.07.010 PMID: 25173134

46. Zhang Q, Yu W, Lee S, Xu Q, Naji A, Le AD. Bisphosphonate Induces Osteonecrosis of the Jaw in Diabetic Mice via NLRP3/Caspase-1-Dependent IL-1beta Mechanism. J Bone Miner Res, 2015. 30(12): p. 2300–12. https://doi.org/10.1002/jbmr.2577 PMID: 26081624

47. Gutta R, Louis PJ. Bisphosphonates and osteonecrosis of the jaws: science and rationale. Oral Surg Oral Med Oral Pathol Oral Radiol Endod, 2007. 104(2): p. 186–93. https://doi.org/10.1016/j.tripleo.2006.12.004 PMID: 17448709

48. Canderelli R, Leccesse LA, Miller NL, Unruh Davidson J. Benefits of hormone replacement therapy in postmenopausal women. J Am Acad Nurse Pract, 2007. 19(12): p. 635–41. https://doi.org/10.1111/j.1745-7599.2007.00269.x PMID: 18042129

49. Kilkenny C, Browne WJ, Cuthill IC, Emerson M, Altman DG. Improving bioscience research reporting: the ARRIVE guidelines for reporting animal research. Vet Clin Pathol, 2012. 41(1): p. 27–31. https://doi.org/10.1111/j.1939-165X.2012.00418.x PMID: 22390425

50. Byers SL, Wiles MV, Dunn SL, Taft RA. Mouse estrous cycle identification tool and images. PLoS One, 2012. 7(4): p. e35538. https://doi.org/10.1371/journal.pone.0035538 PMID: 22514749

51. Cora MC, Kooistra L, Travlos G. Vaginal Cytology of the Laboratory Rat and Mouse: Review and Criteria for the Staging of the Estrous Cycle Using Stained Vaginal Smears. Toxicol Pathol, 2015. 43(6): p. 776–93. https://doi.org/10.1177/0192623315570339 PMID: 25739587

52. Vieira AE, Repeke CE, Ferreira Junior Sde B, Colavite PM, Biguetti CC, Oliveira RC, et al. Intramembranous bone healing process subsequent to tooth extraction in mice: micro-computed tomography, histomorphometric and molecular characterization. PLoS One, 2015. 10(5): p. e0128021. https://doi.org/10.1371/journal.pone.0128021 PMID: 26023920

53. Biguetti CC, Vieira AE, Cavalla F, Fonseca AC, Colavite PM, Silva RM, et al. CCR2 Contributes to F4/80+ Cells Migration Along Intramembranous Bone Healing in Maxilla, but Its Deficiency Does Not Critically Affect the Healing Outcome. Front Immunol, 2018. 9: p. 1804. https://doi.org/10.3389/fimmu.2018.01804 PMID: 30147688

54. Bouxsein ML, Boyd SK, Christiansen BA, Guldberg RE, Jepsen KJ, Müller R. Guidelines for assessment of bone microstructure in rodents using micro-computed tomography. J Bone Miner Res, 2010. 25(7): p. 1468–86. https://doi.org/10.1002/jbmr.141 PMID: 20533309

55. Vivan RR, Mecca CE, Biguetti CC, Rennó AC, Okamoto R, Cavenago BC, et al. Experimental maxillary sinus augmentation using a highly bioactive glass ceramic. J Mater Sci Mater Med, 2016. 27(2): p. 41. https://doi.org/10.1007/s10856-015-5652-7 PMID: 26712707

56. Fakhouri WD, Metwalli K, Naji A, Bakhiet S, Quispe-Salcedo A, Nitschke L, et al. Intercellular Genetic Interaction Between Irf6 and Twist1 during Craniofacial Development. Sci Rep. 2017 Aug 2; 7(1):7129. https://doi.org/10.1038/s41598-017-06310-z PMID: 28769044

57. Thompson J, Mendoza F, Tan E, Gaggar AS, Biguetti C, Fakhouri WD. A cleft lip and palate gene, IRF6, is involved in bone mineralization. Dev. Dyn. 2019, 248(3): 221–232.

58. Advisory Task Force on Bisphosphonate-Related Ostenonecrosis of the Jaws, American Association of Oral and Maxillofacial Surgeons. American Association of Oral and Maxillofacial Surgeons position paper on bisphosphonate-related osteonecrosis of the jaws. J Oral Maxillofac Surg, 2007. 65(3): p. 369–76. https://doi.org/10.1016/j.joms.2006.11.003 PMID: 17307580

59. Flurkey K, Currer JM, Harrison DE. The mouse in aging research, in: Fox JG, et al., (eds.). The Mouse in Biomedical Research. Elsevier: 2nd Edition American College Laboratory Animal Medicine, Burlington, MA 2007, pp. 637–672.

60. The NAMS 2017 Hormone Therapy Position Statement Advisory Panel. The 2017 hormone therapy position statement of The North American Menopause Society. Menopause, 2017. 24(7): p. 728–753. https://doi.org/10.1097/GME.0000000000000921 PMID: 28650869

61. Ervolino E, Statkievicz C, Toro LF, de Mello-Neto JM, Cavazana TP, Issa JPM, et al. Antimicrobial photodynamic therapy improves the alveolar repair process and prevents the occurrence of osteonecrosis of the jaws after tooth extraction in senile rats treated with zoledronate. Bone, 2018. 120: p. 101–113. https://doi.org/10.1016/j.bone.2018.10.014 PMID: 30339908

62. Matsumoto MA, de Abreu Furquim EM, Gonçalves A, Santiago-Júnior JF, Saraiva PP, Cardoso CL, et al. Aged rats under zoledronic acid therapy and oral surgery. J Craniomaxillofac Surg, 2017. 45(5): p. 781–787. https://doi.org/10.1016/j.jcms.2017.02.002 PMID: 28318924

63. Gavalda C, Bagan JV. Concept, diagnosis and classification of bisphosphonate-associated osteonecrosis of the jaws. A review of the literature. Med Oral Patol Oral Cir Bucal, 2016. 21(3): p. e260–70. https://doi.org/10.4317/medoral.21001 PMID: 26827066

64. Curra C, Cardosos CL, Ferreira O Jr, Curi M, Matsumoto MA, Cavenago BC, et al. Medication-related osteonecrosis of the jaw. Introduction of a new modified experimental model. Acta Cir Bras, 2016. 31 (5): p. 308–13. https://doi.org/10.1590/S0102-865020160050000003 PMID: 27275851

65. Gross C, Weber M, Creutzburg K, Möbius P, Preidl R, Amann K, et al. Osteoclast profile of medication-related osteonecrosis of the jaw secondary to bisphosphonate therapy: a comparison with osteoradionecrosis and osteomyelitis. J Transl Med, 2017. 15(1): p. 128. https://doi.org/10.1186/s12967-017-1230-8 PMID: 28587628

66. Terai K, Takano-Yamamoto T, Ohba Y, Hiura K, Sugimoto M, Sato M, et al. Role of osteopontin in bone remodeling caused by mechanical stress. J Bone Miner Res, 1999. 14(6): p. 839–49. https://doi.org/10.1359/jbmr.1999.14.6.839 PMID: 10352091

67. Rogers MJ, Crockett JC, Coxon FP, Mönkkönen J. Biochemical and molecular mechanisms of action of bisphosphonates. Bone, 2011. 49(1): p. 34–41. https://doi.org/10.1016/j.bone.2010.11.008 PMID: 21111853

68. Bonewald LF. The amazing osteocyte. J Bone Miner Res, 2011. 26(2): p. 229–38. https://doi.org/10.1002/jbmr.320 PMID: 21254230

69. Loiselle AE, Jiang JX, Donahue HJ. Gap junction and hemichannel functions in osteocytes. Bone, 2013. 54(2): p. 205–12. https://doi.org/10.1016/j.bone.2012.08.132 PMID: 23069374

70. Okada S, Yoshida S, Ashrafi SH, Schraufnagel DE. The canalicular structure of compact bone in the rat at different ages. Microsc Microanal, 2002. 8(2): p. 104–15. PMID: 12533240

71. Holmbeck K, Bianco P, Pidoux I, Inoue S, Billinghurst RC, Wu W, et al. The metalloproteinase MT1-MMP is required for normal development and maintenance of osteocyte processes in bone. J Cell Sci, 2005. 118(Pt 1): p. 147–56. https://doi.org/10.1242/jcs.01581 PMID: 15601659

72. Bloch SL, Kristensen SL, Sørensen MS. The viability of perilabyrinthine osteocytes: a quantitative study using bulk-stained undecalcified human temporal bones. Anat Rec (Hoboken), 2012. 295(7): p. 1101–8.

73. Marx RE. A decade of bisphosphonate bone complications: what it has taught us about bone physiology. Int J Oral Maxillofac Implants, 2014. 29(2): p. e247–58. https://doi.org/10.11607/jomi.te61 PMID: 24683588

74. Verborgt O, Gibson GJ, Schaffler MB. Loss of osteocyte integrity in association with microdamage and bone remodeling after fatigue in vivo. J Bone Miner Res, 2000. 15(1): p. 60–7. https://doi.org/10.1359/jbmr.2000.15.1.60 PMID: 10646115

75. Verborgt O, Tatton NA, Majeska RJ, Schaffler MB. Spatial distribution of Bax and Bcl-2 in osteocytes after bone fatigue: complementary roles in bone remodeling regulation? J Bone Miner Res, 2002. 17 (5): p. 907–14. https://doi.org/10.1359/jbmr.2002.17.5.907 PMID: 12009022

76. Aguirre JI, Plotkin LI, Stewart SA, Weinstein RS, Parfitt AM, Manolagas SC, et al. Osteocyte apoptosis is induced by weightlessness in mice and precedes osteoclast recruitment and bone loss. J Bone Miner Res, 2006. 21(4): p. 605–15. https://doi.org/10.1359/jbmr.060107 PMID: 16598381

77. Kennedy OD, Herman BC, Laudier DM, Majeska RJ, Sun HB, Schaffler MB. Activation of resorption in fatigue-loaded bone involves both apoptosis and active pro-osteoclastogenic signaling by distinct osteocyte populations. Bone, 2012. 50(5): p. 1115–22. https://doi.org/10.1016/j.bone.2012.01.025 PMID: 22342796

78. Kogianni G, Mann V, Noble BS. Noble, Apoptotic bodies convey activity capable of initiating osteoclastogenesis and localized bone destruction. J Bone Miner Res, 2008. 23(6): p. 915–27. https://doi.org/10.1359/jbmr.080207 PMID: 18435576

79. Wehrhan F, Hyckel P, Guentsch A, Nkenke E, Stockmann P, Schlegel KA, et al. Bisphosphonate-associated osteonecrosis of the jaw is linked to suppressed TGFbeta1-signaling and increased Galectin-3 expression: a histological study on biopsies. J Transl Med, 2011. 9: p. 102. https://doi.org/10.1186/1479-5876-9-102 PMID: 21726429

80. Roelofs AJ, Coxon FP, Ebetino FH, Lundy MW, Henneman ZJ, Nancollas GH, et al. Fluorescent risedronate analogues reveal bisphosphonate uptake by bone marrow monocytes and localization around osteocytes in vivo. J Bone Miner Res, 2010. 25(3): p. 606–16. https://doi.org/10.1359/jbmr.091009 PMID: 20422624